Estimating Poly(N-isopropylacrylamide) size in solution below the LCST using fluorescence correlation spectroscopy with non-covalent bound fluorophores

Polymer Testing 137 (2024) 108500

Contents lists available at ScienceDirect

Polymer Testing

journal homepage: www.elsevier.com/locate/polytest

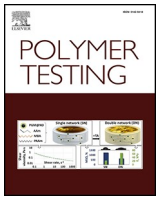

Estimating Poly(N-isopropylacrylamide) size in solution below the LCST using fluorescence correlation spectroscopy with non-covalent bound fluorophores

Camila van Zanten, Alan G. Ryder *

Nanoscale Biophotonics Laboratory, University of Galway, University Road, Galway, H91TK33, Ireland

ARTICLE INFO

Keywords:
Polymer
PNIPAm
Solution
Fluorescence
Size
Fluorescence correlation spectroscopy

ABSTRACT

Accurate size measurements of nanosized polymer chains in dilute solutions is important for understanding polymer behavior, however, these measurements can be challenging to implement accurately, and are technique dependent. Here we explore the use of Fluorescence Correlation Spectroscopy (FCS) to determine the size of single polymer chains in dilute solutions (<2 wt%). FCS, a technique with single molecule sensitivity, generally requires the use of covalently labelled polymers which can distort physicochemical behavior. Here, FCS based size measurements were based on the non-covalent interaction of fluorophores (Alexa 405, Atto 390, and Atto 425) with PNIPAm in water at 25 °C (below the Lower Critical Solution Temperature).

FCS estimated size (hydrodynamic radius) of three different MW PNIPAm samples in water were: 5.0 ± 1.0 nm (28.5 kDa), 5.0 ± 1.0 nm (38 kDa), 3.3 ± 0.5 nm (55.5 kDa), in reasonable agreement with theoretical calculations. Accuracy was directly related to the fraction of PNIPAm-bound fluorophore, which were, for 1 wt% PNIPAm solutions in water: ~11.5 % (Atto 390), ~8.1 % (Atto 425), and 4 % (Alexa 405). This method has several advantages in that it does not require a covalent labelling of PNIPAm, it can be implemented on very small sample volumes, and allows for *in-situ* measurements.

1. Introduction

Knowing the exact size of single polymer chains/particles in solution can be critical for many biomaterials and biopharmaceutical applications where polymers are interacting in solution to generate new entities. In these dilute regimes (<2 % w/w), the use of Dynamic Light Scattering (DLS) can be challenging due to weak light scattering caused by a combination of small refractive index differences between polymer and dispersant, and because of low polymer concentrations. Fluorescence Correlation Spectroscopy (FCS) on the other hand offers nanomolar sensitivity and is widely used to study the solution properties of polymers [1,2], by measuring the diffusion of probes in dilute, semi-dilute, and concentrated polymer regimes using different approaches [3–5]. In semi-dilute and concentrated polymer systems, probe diffusion depends on how its size (e.g., hydrodynamic radius (R_h) or radius of gyration (R_g)), compares to the polymer correlation length, ξ [6] and for polymer solutions, the viscosity that the probe will experience is length-scale dependent [7]. When the diffusing particle is smaller than the correlation length ξ, the particle can move unhindered across the space between polymer chains and the viscosity felt by the probe does not correspond to the macroscopic viscosity of the polymer solution [8–10]. For probe sizes orders of magnitude smaller than ξ (i.e., for molecular probes), the experimentally determined diffusion coefficient is much faster than that predicted by the Stokes-Einstein (SE) relationship[1] when the macroscopic viscosity is used [5]. This breakdown of the SE relationship implies that smaller probes diffuse unhindered through polymer networks, and may experience a local, nano-viscosity instead of the solution's macro-viscosity [6]. If, however, one wants only to look at the diffusion and behaviour of single polymer chains, then one needs to work in the dilute regime (i.e., below the critical concentration, c*), where polymer chain overlap is not expected and only solvent viscosity determines the free probe diffusion rate [8,11]. Additionally, by working with dilute polymer solutions we can circumvent potential measurement artefacts that can arise due to increased viscosity [12,13], as well as additional modes of diffusion characteristic of more complex polymer systems [14,15].

* Corresponding author.
E-mail address: alan.ryder@universityofgalway.ie (A.G. Ryder).

[1] $D = \frac{kT}{6\pi\eta R_h}$, where k is the Boltzmann constant, T is the temperature, and η is the viscosity of the medium.

https://doi.org/10.1016/j.polymertesting.2024.108500
Received 26 March 2024; Received in revised form 5 June 2024; Accepted 20 June 2024
Available online 21 June 2024

When using FCS to determine the size of polymer chains, one can either covalently label polymer chains with a suitable fluorophore, or rely on a non-covalent attractive interaction between polymer and fluorophore. Most FCS experiments on single-chain polymer diffusion use covalent labelling [16–18], which requires a time consuming additional experimental procedure, and also alter the physicochemical properties of the polymer. Thus, non-covalent interactions may be a more convenient measurement approach with minimal impact on polymer behaviour.

FCS was used to study diffusion of labelled polystyrene (PS) single chains in unlabelled PS solutions of identical MW (67 kDa) up to a concentration of 7.0 wt% [19] and it was found that diffusion was unhindered in the dilute regime (<1.0 wt%) for the labelled PS chains. A similar approach using Alexa 488 labelled, polyelectrolyte, poly-methacrylic acid (PMAA*) in dilute unlabelled PMAA buffered solutions, yielded a single diffusion time that did not vary considerably (~14.5–~15.2 $\mu m^2 s^{-1}$) with increasing matrix concentration up to ~1.0 mg/ml after which there was a very large decrease as one approached the crossover concentration, c*, of 1.7 mg/ml [20]. This relatively stable diffusion region was explained by the screening effect of the salts in the buffer and by the small probe size ($R_h = 15$ nm) compared to the much larger polymer chain-to-chain average distances, ξ, 10.6 μm, which meant that diffusion was unhindered. In contrast when the buffer salts are removed, the screening effect decreases, and there is much greater electrostatic interactions generating a much smaller range for the maximum diffusion coefficient, ~7.5 $\mu m^2 s^{-1}$, up to ~10^{-2} mg/ml.

Non-covalent interactions between fluorophores and polymers have been observed by FCS, for example slower diffusion of Atto 488 and Atto 655 in PEG solutions was reported [21] with complexation observed for PEG concentrations as low as 0.1 wt%, and the data suggested that this was a hydrogen bond driven interaction. However, this study only used single species modelling to fit the data and thus no size measurements of the fluorophore-PEG complex were obtained. Electrostatic driven, non-covalent interactions have also been studied by FCS between cationic rhodamine 6G (R6G) and anionic sulfo-rhodamine G in sodium polystyrene sulfonate (PSS) polyelectrolytes [22]. It was reported that for the Rh6G-PSS system, there were at least two components: a fast diffusing component, similar to free Rh6G in water, which remained practically constant over the polymer concentrations studied; and a slow diffusing component, which had a diffusion constant similar to the covalently labelled polymer. Vagias et al. [23], using FCS looked in detail at the complex diffusion of several fluorophores including: Rhodamine 6G and AlexaFluor 647 and 488, with PNiPAAm (N-isopropyl acrylamide) terpolymers. They found, fluorophore slow down at low polymer concentrations and detailed a second, smaller diffusion coefficient related to fluorophore-polymer interactions. They showed that the slow diffusion coefficient versus concentration more closely matched the macromolecular tracer slowdown, and was thus related to polymer size.

The primary purpose of this study was to see if FCS using non-covalent interactions with small molecule Alexa and Atto fluorophores (excitable at 405 nm) could be used to accurately determine the size of PNIPAm in solution, at relatively low solution concentrations, below the LCST.

2. Materials and methods

Materials: Atto 390 carboxylic acid terminated (catalogue No. 89313), Atto 425 carboxylic acid terminated (Cat. # 56759), Sodium dodecyl sulfate (BioXtra, ≥99.0 %) and high purity water (HPW) all were purchased from Sigma-Aldrich, while Alexa Fluor 405 NHS ester (Cat. # A30000) was purchased from ThermoFisher, and all fluorophores were used as received (Fig. S1, supplemental information). Three samples of PNIPAm with different molecular weights (MW) were purchased from Sigma-Aldrich and used as received: ~30 kDa, catalogue No. 806471, Certificate of Analysis (CoA) specifies 28.47 kDa (white powder); 20–40 kDa, #535311, CoA specifies 38.245 kDa; ~40 kDa, #535311, CoA specifies 55.488 kDa (white powder). The last material was specified on the CoA as being crystalline powder, but it visually appears to be an amorphous powder. The CoA sizes were determined by gel permeation chromatography according to the manufacturer.

Sample preparation: For FCS measurements, PNIPAm stock solutions were prepared in advance (stored at 2–8 °C) at either 2.0 or 4.0 wt % in HPW, and diluted as required to prepare the fluorophore-PNIPAm solutions fresh on the day of measurement. The following PNIPAm concentrations were used: *i).* Atto390-PNIPAm (28.5 kDa) system: 0.02, 0.05, 0.1, 0.2, 0.5, and 1.0 wt%; *ii).* Alexa 405-PNIPAm (38 kDa) system: 0.02, 0.05, 0.1, 0.2, 0.5, 0.75, 1.0, 1.5, 2.0, 2.5, and 3.0 wt%; and *iii).* Atto 425-PNIPAm (55.5 kDa) system: 1.0 wt%. All fluorophore-PNIPAm solutions contained 10 nM fluorophore. Stock fluorophore solutions were made up as follows: The contents of a sealed vial containing the fluorophore were dissolved in 200 μL of an appropriate solvent (acetonitrile for Atto 390/425 and water for Alexa 405). These pre-dissolved fluorophores were then made up to 25 mL (Atto 390) or 50 mL (Atto 425 and Alexa 405) final volumes with HPW. Stock solution concentration was determined by absorbance spectroscopy, using the manufacturer provided molar absorption coefficients: Atto 390, $\varepsilon_{390} = 2.4 \times 10^4\ M^{-1}\ cm^{-1}$, Atto 425 $\varepsilon_{439} = 4.5 \times 10^4\ M^{-1}\ cm^{-1}$, and Alexa 405 $\varepsilon_{401} = 3.5 \times 10^4\ M^{-1}\ cm^{-1}$ and was found to be 122 μM (Atto 390), 30 μM (Atto 425), and 19 μM (Alexa 405).

Instrumentation: FCS measurements were made with an Alba fluorescence fluctuation spectroscopy system (ISS, Champaign Illinois) fitted to an inverted Olympus IX71 microscope equipped with a 405 nm excitation source and a × 60 water objective with a correction collar, as previously described [24]. Laser power was monitored with a power meter positioned just above the objective lens, prior to the first measurement and after the last measurement each day. It was found that the system required ~40 min for the power output to stabilize. Laser power was adjusted according to the fluorophore type, with Alexa 405 containing samples using 12 ± 1 μW, whereas for samples containing Atto fluorophores a lower power was used ~6.5 ± 1 μW. Confocal volume was calibrated daily by using a 10 nM solution of Alexa 405, whose diffusion coefficient was determined in our laboratory to be 333 ± 16 $\mu m^2/s$ [24]. The resulting autocorrelation function (ACF) used for calibration was fitted by fixing Alexa 405's diffusion coefficient and concentration, such that w_0 and z_0 were allowed to vary. These parameters were then determined to be: $w_0 = 0.38$ μm and $z_0 = 2.1$ μm, yielding a structural parameter $k = z_0/w_0 = 5.5$, which is within the expected 2 to 6 range [25]. These w0 and z0 values were used for all FCS fitting unless otherwise noted. For sample measurements, 300 μL of each solution were loaded into an 8 well chambered cover slide (Nunc® Lab-Tek® II Chamber Slide™). These were then mounted onto the microscope stage and focus adjusted to a fixed point 100 μm within the solution. Two or 5-min measurements in triplicate were done on each sample. FCS data were analysed using the ISS Alba analysis software (VistaVision ver. 4.2.148).

FCS Data Analysis: The simplest model function represents one species freely diffusing within a femto-litre sized volume, which is described by a 3D Gaussian function and the ACF can be expressed as [26]:

$$G(t) = \frac{1}{N} \frac{1}{\left(1 + \frac{1}{\tau_D}\right)\left(1 + \frac{1}{k^2 \tau_D}\right)^{1/2}} \quad (1)$$

Where N is the average number of molecules in the sampling volume, τ_D is the diffusion time of the species, and k is the structural parameter, or eccentricity of the confocal volume, which represents the ratio of the axial by the lateral radii z_0 and w_0, respectively, by $k = \frac{z_0}{w_0}$. For two or more freely diffusing species which may or may not have the same molecular brightness (which is contained in the quantum yield term, Q),

the ACF can be expressed as [26]:

$$G(t) = \frac{1}{(\sum Q_k N_k)^2} \sum Q_j^2 N_j \left(1 + \frac{t}{\tau_{Dj}}\right)^{-1} \left(1 + \frac{t}{k^2 \tau_{Dj}}\right)^{-1/2} \quad (2)$$

Where Q_j and N_j are the quantum yield and average number of molecules of species j, and k represents the index of summation.

3. Results & discussion

The different PNIPAm samples used were sourced commercially and originally used for making polymer thin films and investigating PNIPAm-protein interactions. It is particularly important to know precise polymer sizes in solution as this helps better understand their physiochemical properties and for optimizing reactions/interactions with proteins. The size and shape that individual polymer chains adopt in solution depend, amongst other factors, on the type of solvent system [27] and on the polymer molecular weight [16,28].

Solution polymer properties were modelled and predicted (Table 1) using simulations and scaling laws [29–32]. This showed that the correlation length ξ (and expected R_h) of PNIPAm was much larger than that of the fluorophores, so we do not expect any anomalous behaviour with the FCS measurements.

FCS measurements: The PNIPAm used for the FCS measurements were between 2 and 4 years after the date of manufacture, but had been acquired new for these experiments from the manufacturer. The accurate sizing of polymer NPs in solution by FCS often makes use of the Stokes-Einstein relationship, of which a crucial parameter is the viscosity η experienced by the fluorophore [3–5]. The importance of determining the accurate viscosity to use in the Stokes-Einstein relationship stems from the fact that serious deviations from the computed values can be expected dependent on whether the probe "feels" a nano- or macro-viscosity [3,7,35]. Thus, we had to first measure the impact of polymer concentration on the diffusion of Alexa 405, and this was done with PNIPAm concentrations of 0.5, 0.75, 1.0, 1.5, 2.0, 2.5, and 3.0 wt%. These concentrations were selected to be below the critical overlap concentration, c^*, which for 40 kDa PNIPAm was ~5 wt% (Table 1), to try and ensure that only single chains were present in solution.

Fig. 1A shows representative autocorrelation functions for Alexa 405 in water, 3.0 wt% PNIPAm, and in a 50 % glycerol:water mixture while Fig. 1B shows the changing diffusion coefficient with increasing glycerol content or PNIPAm concentration. The effect of glycerol on fluorophore diffusion is clearly a case of slower diffusion due to higher solution viscosity (we had taken into account the changing refractive index using the correction collar on the objective for these measurements, [24]). The slower Alexa diffusion with increasing PNIPAm concentration could be due to macromolecular crowding arising from the dissolved polymer but this is unlikely because the concentrations were all below the critical concentration (Table 1). In an attempt to determine whether this was a measurement artefact or an actual case of diffusion slowdown, we looked at the average apparent number of molecules, *N*, within the confocal volume against PNIPAm concentration for a fixed focal position. For viscous and crowded solutions where samples can experience excessive light scattering, the apparent *N* of the fluorophore species may increase over that compared to its value in pure solvent [36,37]. This is seen for Alexa 405 in glycerol:water mixtures (Fig. 2), which is consistent with a distortion of the focal volume due to a change in the degree of light scattering [36]. This could be caused by either the presence of large particles or a change in focus induced by varying refractive index. Here the clear increase in N was most likely caused by an increase (by ~4 %) in refractive index at higher glycerol concentrations [24].

This variation in the apparent *N* for Alexa 405 and Atto 390 in PNIPAm solutions of varying concentrations showed very different behaviour, using the same instrumental conditions. The PNIPAm solutions yielded a fairly constant *N* across the range of polymer concentrations tested, which indicates that there were no issues with refractive index or light scattering changes over the concentration ranges investigated. The sharp increase in *N* for Atto 390 in 2.0 wt% PNIPAm was most likely due to an increase in Atto 390 molecules in solution, as shown in Tables S–1 (SI). In the absence of polymer, or at low PNIPAm concentrations, the relatively hydrophobic Atto 390 seems to adsorb onto the container surfaces (more than the other fluorophores), reducing

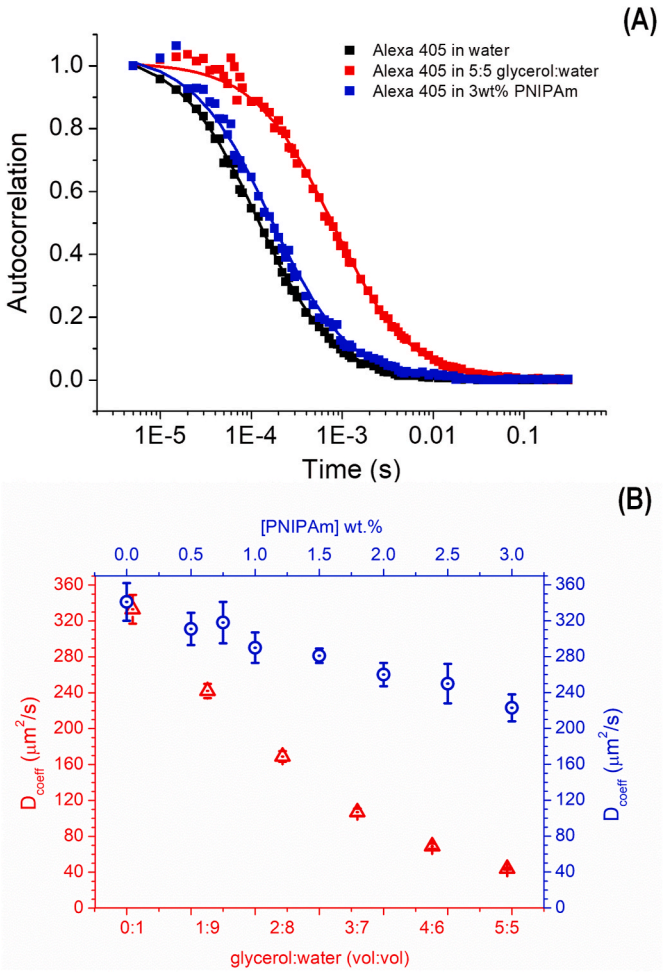

Fig. 1. ***A).*** Effect of the addition of either PNIPAm (to a final concentration of 3.0 wt%) or glycerol (50 vol%) to water on the diffusion time of Alexa 405, as seen by the shift in the ACFs to the right. ***B).*** Comparison between D_{coeff} values derived from a one species diffusion model fitting for 10 nM Alexa 405 in glycerol:water mixtures (triangles) and in 0 → 3.0 wt% PNIPAm (38 kDa) solutions (circles). Data points represent the average of three measurements.

Table 1
Theoretically calculated molecular weight (MW) dependent solution parameters of PNIPAm polymers and fluorophores. Hydrodynamic radius (R_h), Radius of gyration (R_g), critical overlap concentration (c*), and correlation length (ξ).

Sample	MW (kDa)	R_h (nm)[a]	R_g (nm)[a]	c* (wt%)[b]	ξ (nm)[c]
Alexa 405	1.03			n/a	0.6
Atto 390	0.343			n/a	0.5
Atto 425	0.402			n/a	0.5
PNIPAm	28.5	4.1	5.7	6.1	22.1
PNIPAm	38	4.8	6.7	5.3	23.2
PNIPAm	55.5	5.8	8.2	4.3	24.4

[a] Calculated from Ref. [33] using PNIPAm materials with MW > 130 kDa and at 20 °C.
[b] Calculated from ref. [34].
[c] Calculated from Ref. [3], using $x = 0.01$ g/mL (1.0 wt%).

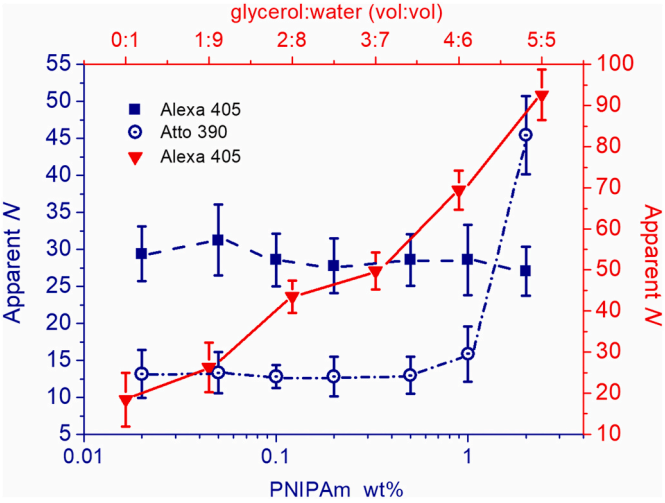

Fig. 2. Effect of increasing of glycerol (red) or PNIPAm (blue) concentration on the apparent number of molecules N recovered for Alexa 405 and Atto 390. Fluorophore concentration was 10 nM in all solutions, and each data point represent the average of 9 measurements, error bars are the standard deviation. All FCS data in this figure was collected at the same fixed focal depth and without the use of a correction collar. Connecting lines are only visual aids.

its solution concentration by nearly 60 %. This non-specific binding of fluorophores to polymer and glass surfaces[2] is well known [38,39] and the use of coatings, such as polyethylene glycol (PEG), have been shown to inhibit fluorophore adsorption to surfaces [40]. Here, it looks like PNIPAm had a similar effect, absorbing onto all of the container surfaces at sufficiently high concentrations, thus preventing Atto 390 non-specific adsorption or displacing any previously bound fluorophores.

When we looked at the effect of PNIPAm concentration on the FCS data fitting, we found that a one species diffusion model described accurately both Alexa 405/PNIPAm and Atto 390/PNIPAm systems well up to ~0.2 wt%, but above this the model broke down (Fig. S2/S3, Table S-2, SI). This is seen by the fact that the D_{coeff} recovered no longer corresponded to that of the freely diffusing fluorophore in water. Above 0.5 wt% PNIPAm, a two species diffusion model was more appropriate as seen by comparing the residuals of the two models (Figs. S3 and SI). This coupled with the fact that slowdown effects on the fluorophore's diffusion due to polymer crowding is not present (Fig. 2), we hypothesised that the measured effects were due to the presence of both free and polymer bound fluorophore in solution. The second species recovered was assumed to be PNIPAm-bound fluorophores (D_{bound} [21–23]), and this species was observed, at varying levels, for all three systems. The Atto 425/PNIPAm system was the last system studied, and only one concentration was used based on results from the other fluorophores. Fig. 3A shows the recovered diffusion coefficients for Alexa 405 and Atto 390 in the 38 and 28.5 kDa PNIPAm solutions, and the clear differences between the two polymers of different MW. Fig. 3B, shows the overlap between a tracer diffusion master curve (as defined in Ref. [18]) and the measured diffusion component, D_{free}, of the freely diffusing fluorophore components. The almost perfect overlap suggests that there is no macromolecular crowding induced diffusion slowdown up to 2.0 wt% PNIPAm. Beyond this point, a slowdown governed by polymer concentration would be expected (as shown by the sharp curve decay in the right hand side of Fig. 3B) [18,23].

Table 2 shows the FCS parameters recovered for the fluorophore/PNIPAm systems and this shows that Alexa 405 formed a much weaker

[2] In our case, this likely arose from adsorption of the fluorophore to the polystyrene walls and borosilicate glass floor of the sample chambers.

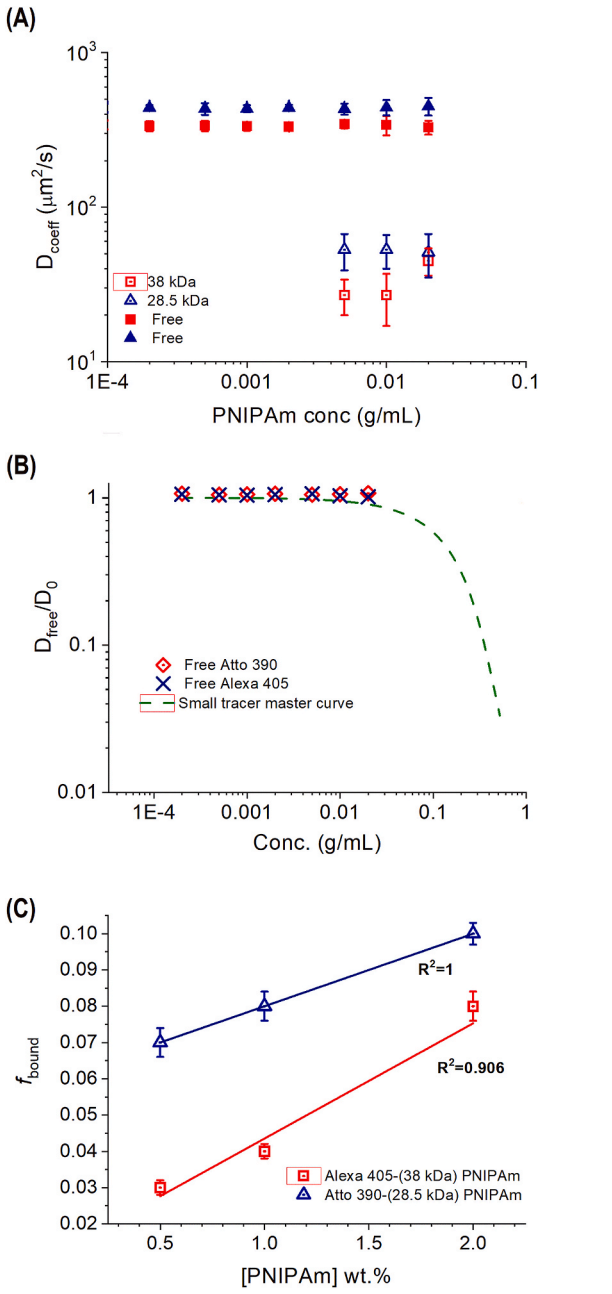

Fig. 3. ***(A).*** D_{free} and D_{bound} recovered from a two species fit for Alexa 405/PNIPAm (38 kDa, squares) and Atto 390-PNIPAm (28.5 kDa, triangles), with varying PNIPAm concentrations; ***(B).*** Normalized D_{free}, derived from the two species diffusion model fitting, of Alexa 405 and Atto 390 in PNIPAm solutions. D_0 is the diffusion coefficient of the fluorophore in pure water: 333 μm²/s (Alexa 405) and 440 μm²/s (Atto 390). The dashed line is the master diffusion curve for Alexa 405 [18]; ***(C).*** Recovered fractions, f_{bound}, of PNIPAm-bound fluorophore, for Alexa 405 and Atto 390. Data points are average from 9 measurements with error bars being the standard deviation.

complex with the larger, slower diffusing species only being observed at >0.5 wt%. The Atto fluorophores did bind better but these fluorophores photobleached more significantly than Alexa 405 [24]. The 28.5 kDa and 38 kDa PNIPAm samples were both the same size, 5 ± 1 nm, and close to the calculated values (Table 1). Atto 425/PNIPAm (55.5 kDa) yielded the smallest R_h value of 3.3 ± 0.5 nm which is similar to values reported in the literature for lower MW polymers in water. For example, freshly prepared and purified PNIPAm (MW ~32.7 kDa and 21.4 kDa) in water, R_h of ~4 and 3 nm were determined by FCS with covalently

Table 2
FCS results from one- and two-species fitting of fluorophore (Alexa 405, Atto 390, and Atto 425)/PNIPAm mixtures in solution. For the two species fit, D_{free} was fixed for each fluorophore. R_h values were calculated using D_{bound} values with the Stokes-Einstein relationship. Data generated using a minimum of 9 replicate measurements.

Sample	[PNIPAm] wt%	D_{free} ($\mu m^2/s$)	F_{bound} %	D_{bound} ($\mu m^2/s$)	PNIPAm R_h (*nm*)
Atto 425/ PNIPAm 55.5 kDa	1	438[a]	11.5 ± 0.5	67 ± 9 (13 %)	3.3 ± 0.5
Atto390/ PNIPAm 28.5 kDa	0	436 ± 29	–	–	–
	0.02	440 ± 17	–	–	–
	0.05	433 ± 38	–	–	–
	0.1	434 ± 23	–	–	–
	0.2	440 ± 19	–	–	–
	0.5	440[a]	7.0 ± 0.4	53 ± 14 (26 %)	4 ± 1
	1		8.1 ± 0.4	47 ± 18 (38 %)	5 ± 2
	2		10.2 ± 0.3	51 ± 16 (31 %)	5 ± 1
Alexa405/ PNIPAm 38 kDa	0	341 ± 21		–	–
	0.02	335 ± 25	–	–	–
	0.05	336 ± 26	–	–	–
	0.1	334 ± 22	–	–	–
	0.2	331 ± 11	–	–	–
	0.5	333[a]	3.2 ± 0.3	30 ± 7 (23 %)	9 ± 4
	1		4.0 ± 0.4	26 ± 7 (27 %)	9 ± 2
	2		8.1 ± 0.4	45 ± 9 (20 %)	5 ± 1

[a] These values represent the diffusion coefficient of the free fluorophore, which were used as fixed parameters in the two species diffusion model fitting.

labelled probes [16].

Our 38 kDa sample is a bit bigger than their 32.7 kDa (N290 in Ref. [16]) sample (5 ± 1 nm vs ~4.2 nm) with a slightly slower diffusion time 45 versus 50 μms^{-1}, but overall these are in good agreement. Our 55 kDa is significantly smaller than predicted (Table 1) whereas our 28.5 kDa sample is also larger than their 32.8 kDa (N290) sample. As the pattern is not consistent, we can probably discount either multiply bound probes or hydrogen bond mediated contraction. It is, therefore, most likely that sample provenance and quality is the difference here. Wang et al.'s samples [16] were freshly synthesized and carefully purified whereas our samples were acquired from a vendor and used as supplied. It is also important to note that the 28.5 (manufactured in 2015) and 38 (manufactured in 2016) kDa samples were 1–2 years older than the 55 kDa material (manufactured in 2017), and probably originated from different manufacturing/purification processes. A DLS examination of these materials several years later showed very different, and larger particle sizes which we attribute to solid state aging [41,42].

There are two other factors to note. First, the poorer resolution of our measurements compared to covalently labelled systems, is related to the lower fluorophore-polymer binding strengths, and this coupled with FCS repeatability (no better than ±7 %) and poor day-to-day reproducibility (Tables S-2/S-3, SI), and thus size values have an error of at least ±1.0 nm. A second is that this FCS method may tend to bias the fit and misestimate size because of the presence of an excess of unbound fluorophore.

Binding strength: The relationship between weakly bound species and the resolvability of FCS was explored by Vagias et al. [23], and they explained that any given process can only be evaluated by FCS when the length scale L is greater than the beam radius w_0. There are cases with a weak attraction between fluorophore and polymer and in such cases, L_{bound} (polymer bound-fluorophore) and L_{free} (free fluorophore) < w_0, such that the fluorescent probe "hops" between the bound and free states during measurements, making it impossible to distinguish these two states. The binding strength will also affect the equilibrium between bound/unbound fluorophores. Smaller F_{bound} values were consistently recovered for Alexa 405 (~3–4%) compared to Atto 390 or 425 (7–11 %) at the same PNIPAm concentrations (Fig. 3C). The fluorophore/polymer interaction is probably hydrogen bond driven as the NIPAm monomer has a single hydrogen bond donor (the amide hydrogen) and acceptor (the carbonyl group), while the fluorophores have: 1 and 7 (Atto 425), 1 and 5 (Atto 390), and 3 and 15 (Alexa 405) donor (nitrogen atoms) and acceptor (oxygen and nitrogen atoms) sites respectively (numbers obtained from data available at: https://pubchem.ncbi.nlm.nih.gov/). As the 55.5 kDa PNIPAm has ~486 monomers, this provides many sites for hydrogen bonding. Because the fluorophores all have more hydrogen bond acceptors it seems logical that the predominant interaction is hydrogen bond donation from the polymer to the fluorophore. Looking at the 3D structures of the Atto fluorophores also shows that the H-bond donor sites are not very accessible for a bulky polymer molecule. The greater number of acceptor moieties on Atto 425 could thus explain its stronger interaction compared to Atto 390 considering that they have similar chemical structures. Alexa 405 has the same ratio of H-bond donors to acceptors (1:5) as Atto 390 but with larger numbers (3:15) and a significantly different structure. The H-bonding interaction is different, and probably determined by fluorophore steric considerations rather than polymer size explaining why it has a weaker interaction.

There was a minimum concentration (~0.5 wt%, Table 2), below which binding could not be measured accurately [43] and the second species was only observed >0.5 wt% PNIPAm where for Alexa 405 the bound fraction was ~3–4%. Taking into consideration the 10 nM Alexa 405 initial concentration, the concentration of PNIPAm-bound Alexa 405 in solution would be ~0.3 nM, which is probably at the limit of our FCS instrumentation. The anomalies in measured sizes (Table 2) are directly related to the magnitude of the bound fraction, which represents the magnitude of the true signal available for fitting. For F_{bound} values of ~5 %, the corresponding D_{bound} values were biased towards slower diffusing species generating larger than expected sizes. This is probably a fitting process artefact and represents the FCS resolution limit. Accuracy might improve by increasing the number of replicate measurements and using a global fitting approach, but operationally it might be better to use stronger binding fluorophores. Another issue here, is the repeatability and reproducibility of FCS measurements, here repeatability was ~7 % at best (n = 9 measurements), but for the two species fits the errors in F_{bound} values varied and were up to 40 %. This suggests that a more robust tactic would be to take a statistical approach with many replicate measurements, each modelled individually and then statistically analysed. Overall, it is the F_{bound} magnitude that is critical for accurate size measurement, and therefore the measurements with F_{bound}< 5 % were the least accurate and, it would be advisable to have >10 % to ensure a reasonably accurate size value.

4. Conclusions

Leveraging the non-covalent interaction between PNIPAm and fluorophores with FCS measurements we were able to estimate the size (R_h) of single PNIPAm particles in solution at concentrations >0.5 wt%. The attraction of Atto 390 and Atto 425 for PNIPAm was stronger than Alexa 405, as reflected by a higher fluorophore-polymer bound fraction (F_{bound}) of ~8–11 %, and thus these Atto fluorophores were more

suitable for PNIPAm sizing [2,44], however, this has to be balanced with the fact that these photobleached more than Alexa 405 [24]. The FCS determined PNIPAm R_h sizes (MWs 28.5, 38, and 55.5 kDa) were between 3.3 and 5 ± 1 nm and were in good agreement with the theoretically calculated values, indicating that there were single PNIPAm chains in solution, and with some reported literature values (between 3.5 and 5.2 nm) for polymers of similar MW [16,18,45].

A major advantage of this FCS approach is the elimination of time-consuming and often cumbersome polymer labelling and purification steps. Provided that the interaction between fluorophore and polymer is attractive, and generates a large enough fraction of bound fluorophores, this could be used to determine polymer size for dilute polymer solutions without the need for covalent labelling. Improving the limits of detection and quantification to work in more dilute solutions does, however, require the use of stronger binding fluorophores, and a move to a more statistical approach to data analysis by making significantly more replicate measurements to improve data fitting quality. Another advantages of this type of FCS method over more conventional DLS measurements lies in the fact that the sample volumes required can be much lower (<100 μL) and that it can be used for in-situ measurements on or near surfaces. Therefore, despite FCS being more expensive and time consuming, the method enables: minimising the effects of polymer-polymer interactions, measurements on very small amounts and volumes of sample, and on micron sized length scales.

CRediT authorship contribution statement

Camila van Zanten: Writing – original draft, Methodology, Investigation, Formal analysis. **Alan G. Ryder:** Writing – review & editing, Writing – original draft, Supervision, Resources, Funding acquisition, Data curation, Conceptualization.

Declaration of competing interest

The authors declare that they have no known competing financial interests or personal relationships that could have appeared to influence the work reported in this paper.

Data availability

Data will be made available on request.

Acknowledgments

This publication has emanated from research supported in part by a research grant from CAPES (Grant No. BEX 1415-15-8 to CVZ) and from Science Foundation Ireland (SFI) which was co-funded under the European Regional Development Fund under Grant number (14/IA/2282, Advanced Analytics for Biological Therapeutic Manufacture, to AGR). The FCS system was funded by an Irish Health Research Board Equipment Grant (EQ/2004/29). Dzmitry Melnikau is thanked for his assistance with the FCS experiments. The authors declare that there are no conflicts of interest.

Appendix A. Supplementary data

Supplementary data to this article can be found online at https://doi.org/10.1016/j.polymertesting.2024.108500.

References

[1] C.M. Papadakis, P. Košovan, W. Richtering, D. Wöll, Polymers in focus: fluorescence correlation spectroscopy, Colloid Polym. Sci. 292 (2014) 2399–2411.
[2] D. Wöll, Fluorescence correlation spectroscopy in polymer science, RSC Adv. 4 (2014) 2447–2465.
[3] R. Holyst, A. Bielejewska, J. Szymanski, A. Wilk, A. Patkowski, J. Gapinski, A. Zywocinski, T. Kalwarczyk, E. Kalwarczyk, M. Tabaka, N. Ziebacz, S. A. Wieczorek, Scaling form of viscosity at all length-scales in poly(ethylene glycol) solutions studied by fluorescence correlation spectroscopy and capillary electrophoresis, Phys. Chem. Chem. Phys. 11 (2009) 9025–9032.
[4] S.A. Egorov, Anomalous nanoparticle diffusion in polymer solutions and melts: a mode-coupling theory study, J. Chem. Phys. 134 (2011).
[5] A. Tuteja, M.E. Mackay, Breakdown of the continuum Stokes-einstein relation for nanoparticle diffusion, Nano Lett. 7 (2007) 1276–1281.
[6] S.A. Egorov, Anomalous nanoparticle diffusion in polymer solutions and melts: a mode-coupling theory study, J. Chem. Phys. 134 (2011) 084903.
[7] N. Ziebacz, S.A. Wieczorek, T. Kalwarczyk, M. Fialkowski, R. Holyst, Crossover regime for the diffusion of nanoparticles in polyethylene glycol solutions: influence of the depletion layer, Soft Matter 7 (2011).
[8] A. Wisniewska, K. Sozanski, T. Kalwarczyk, K. Kedra-Krolik, C. Pieper, S. A. Wieczorek, S. Jakiela, J. Enderlein, R. Holyst, Scaling of activation energy for macroscopic flow in poly(ethylene glycol) solutions: entangled-Non-entangled crossover, Polymer 55 (2014) 4651–4657.
[9] D. Langevin, F. Rondelez, Sedimentation of large colloidal particles through semidilute polymer solutions, Polymer 19 (1978) 875–882.
[10] P. Tong, X. Ye, B.J. Ackerson, Sedimentation of colloidal particles through a polymer solution, Phys. Rev. Lett. 79 (1997) 2363–2366.
[11] M. Kruger, M. Rauscher, Diffusion of a sphere in a dilute solution of polymer coils, J. Chem. Phys. 131 (2009) 094902.
[12] K. Chattopadhyay, S. Saffarian, E.L. Elson, C. Frieden, Measuring unfolding of proteins in the presence of denaturant using fluorescence correlation spectroscopy, Biophys. J. 88 (2005) 1413–1422.
[13] E. Banachowicz, A. Patkowski, G. Meier, K. Klamecka, J. Gapinski, Successful FCS experiment in nonstandard conditions, Langmuir 30 (2014) 8945–8955.
[14] R.A. Omari, A.M. Aneese, C.A. Grabowski, A. Mukhopadhyay, Diffusion of nanoparticles in semidilute and entangled polymer solutions, J. Phys. Chem. B 113 (2009) 8449–8452.
[15] L. Masaro, X.X. Zhu, Physical models of diffusion for polymer solutions, gels and solids, Prog. Polym. Sci. 24 (1999) 731–775.
[16] F. Wang, Y. Shi, S. Luo, Y. Chen, J. Zhao, Conformational transition of poly(N-isopropylacrylamide) single chains in its cononsolvency process: a study by fluorescence correlation spectroscopy and scaling analysis, Macromolecules 45 (2012) 9196–9204.
[17] J. Pánek, L. Loukotová, M. Hrubý, P. Štěpánek, Distribution of diffusion times determined by fluorescence (lifetime) correlation spectroscopy, Macromolecules 51 (2018) 2796–2804.
[18] T. Cherdhirankorn, A. Best, K. Koynov, K. Peneva, K. Muellen, G. Fytas, Diffusion in polymer solutions studied by fluorescence correlation spectroscopy, J. Phys. Chem. B 113 (2009) 3355–3359.
[19] H. Zettl, U. Zettl, G. Krausch, J. Enderlein, M. Ballauff, Direct observation of single molecule mobility in semidilute polymer solutions, Phys. Rev. 75 (2007) 061804.
[20] D. Pristinski, V. Kozlovskaya, S.A. Sukhishvili, Fluorescence correlation spectroscopy studies of diffusion of a weak polyelectrolyte in aqueous solutions, J. Chem. Phys. 122 (2005) 014907.
[21] Y. Chehreghanianzabi, S.P. Zustiak, Study of polyethylene glycol-fluorophore complex formation by fluorescence correlation spectroscopy, Macromol. Res. 24 (2016) 995–1002.
[22] P. Jia, Q. Yang, Y. Gong, J. Zhao, Dynamic exchange of counterions of polystyrene sulfonate, J. Chem. Phys. 136 (2012) 084904.
[23] A. Vagias, R. Raccis, K. Koynov, U. Jonas, H.J. Butt, G. Fytas, P. Kosovan, O. Lenz, C. Holm, Complex tracer diffusion dynamics in polymer solutions, Phys. Rev. Lett. 111 (2013) 088301.
[24] C. van Zanten, D. Melnikau, A.G. Ryder, Effects of viscosity and refractive index on the emission and diffusion properties of Alexa fluor 405 using fluorescence correlation and lifetime spectroscopies, J. Fluoresc. 31 (2021) 835–845.
[25] V.B.S. Ruttinger, B. Kramer, R. Erdmann, R. Macdonald, F. Koberling, Comparison and accuracy of methods to determine the confocal volume for quantitative fluorescence correlation spectroscopy, J. Microsc. 232 (2008) 343–352.
[26] O. Krichevsky, G. Bonnet, Fluorescence correlation spectroscopy: the technique and its applications, Rep. Prog. Phys. 65 (2002) 251–297.
[27] M.O. Steinhauser, S. Hiermaier, A review of computational methods in materials science: examples from shock-wave and polymer physics, Int. J. Mol. Sci. 10 (2009) 5135–5216.
[28] B. Briscoe, P. Luckham, S. Zhu, Rheological properties of poly(ethylene oxide) aqueous solutions, J. Appl. Polym. Sci. 70 (1998) 419–429.
[29] W. Jiang, J. Huang, Y. Wang, M. Laradji, Hydrodynamic interaction in polymer solutions simulated with dissipative particle dynamics, J. Chem. Phys. 126 (2007) 044901.
[30] J. Klein, The self-diffusion of polymers, Contemp. Phys. 20 (1979) 611–629.
[31] P.E. Rouse, A theory of the linear viscoelastic properties of dilute solutions of coiling polymers, J. Chem. Phys. 21 (1953) 1272.
[32] W. Hess, Self-diffusion and reptation in semidilute polymer solutions, Macromolecules 19 (1986) 1395–1404.
[33] K. Kubota, S. Fujishige, I. Ando, Solution properties of poly(N-isopropylacrylamide) in water, Polym. J. 22 (1990) 15–20.
[34] Q. Ying, B. Chu, Overlap concentration of macromolecules in solution, Macromolecules 20 (1987) 362–366.
[35] K. Koynov, H. Butt, Particle and tracer diffusion in complex liquids, AIP Conf. Proc. 1518 (2013) 357.
[36] H. Engelke, I. Dorn, J.O. Radler, Diffusion and molecular binding in crowded vesicle solutions measured by fluorescence correlation spectroscopy, Soft Matter 5 (2009) 4283–4289.

[37] S. Lehmann, S. Seiffert, W. Richtering, Refractive index mismatch can misindicate anomalous diffusion in single-focus fluorescence correlation spectroscopy, Macromol. Chem. Phys. 216 (2015) 156–163.
[38] Z. Zhang, D. Yomo, C. Gradinaru, Choosing the right fluorophore for single-molecule fluorescence studies in a lipid environment, Biochim. Biophys. Acta 1859 (2017) 1242–1253.
[39] L.C. Zanetti-Domingues, M.L. Martin-Fernandez, S.R. Needham, D.J. Rolfe, D. T. Clarke, A systematic investigation of differential effects of cell culture substrates on the extent of artifacts in single-molecule tracking, PLoS One 7 (2012) e45655.
[40] D.K. Turner, A.E. Wayman, C.N. Rolando, P. Dande, P.W. Carter, E.E. Remsen, Reduction of artifacts in fluorescence correlation spectroscopy due to sample adsorption on optical glass surfaces, Appl. Spectrosc. 67 (2013) 692–698.
[41] M.A. de Castro, A.G. Ryder, Analysing storage and stirring induced aggregation of Poly(N-isopropylacrylamide) using Dynamic Light Scattering, 2024. Submitted.
[42] A. Czerniecka-Kubicka, I. Zarzyka, M. Pyda, Long-term physical aging tracked by advanced thermal analysis of poly(N-isopropylacrylamide): a smart polymer for drug delivery system, Molecules 25 (2020) 3810.
[43] U. Meseth, T. Wohland, R. Rigler, H. Vogel, Resolution of fluorescence correlation measurements, Biophys. J. 76 (1999) 1619–1631.
[44] S.P. Zustiak, R. Nossal, D.L. Sackett, Hindered diffusion in polymeric solutions studied by fluorescence correlation spectroscopy, Biophys. J. 101 (2011) 255–264.
[45] K.L. Linegar, A.E. Adeniran, A.F. Kostko, M.A. Anisimov, Hydrodynamic radius of polyethylene glycol in solution obtained by dynamic light scattering, Colloid J. 72 (2010) 279–281.